Celestial Mechanics and Dynamical Astronomy (2006) 95:371–390
DOI 10.1007/s10569-006-9020-2

ORIGINAL ARTICLE

Weak stability boundary trajectories for the deployment of lunar spacecraft constellations

Christian Circi · Paolo Teofilatto

Received: 7 November 2005 / Revised: 17 March 2006 /
Accepted: 1 April 2006 / Published online: 15 August 2006

Abstract Suitable lunar constellation coverage can be obtained by separating the satellites in inclinations and node angles. It is shown in the paper that a relevant saving of velocity variation ΔV can be achieved using weak stability boundary trajectories. The weakly stable dynamics of such transfers allows the separation of the satellites from the nominal orbit to the required orbit planes with a small amount of ΔV. This paper also shows that only one different set of orbital parameters at Moon can be reached with the same ΔV manoeuvre starting from a nominal trajectory and ending at a fixed periselenium altitude. In fact, such a feature is proved to be common to other simpler dynamical systems, such as the two- and three-body problems.

Keywords Restricted three- and four-body problem · Weak stability lunar transfer · Lunar constellation

1 Introduction

Lunar constellation missions are foreseen in the future to study the lunar environment at various latitudes and longitudes particularly on the side facing away from the Earth. Observations of the lunar polar region are also of particular interest in view of the development of a future lunar base (Bussey and Spudis, 2005). Then it is of interest to consider a lunar constellation with polar orbits to observe the polar regions and inclined orbits for scientific uses. Global coverage can be obtained by varying the orbit inclination or the right ascension of ascending node (Ω). In this paper, a combined variation of two parameters is proposed to achieve global coverage. For example, global coverage can be achieved with three spacecraft is equally spaced on the polar orbit $i_1 = 90°$ and node angle $\Omega_1 = 0°$, and three spacecrafts equally spaced on an orbit with

C. Circi (✉)· P. Teofilatto
Department of Aerospace and Astronautics Engineering, School of Aerospace Engineering, University of Rome, Via Eudossiana 16, Rome, 00184, Italy
e-mail: christian.circi@unirom1.it

$i_2 = 55°$, $\Omega_2 = 140°$. The orbits of all six spacecrafts are circular with radius 3,738 km. However, such a high altitude (2,000 km) could be incompatible with the payload characteristics. If a low altitude is required, the satellites can be set in orbits of radius $R = 1{,}938$ km (Graziani, 2005). The coverage will no longer be global and continuous, but with seven satellites in polar orbit and five satellites at inclination of 55° continuous local coverage, in the polar and 55° latitude band, can be ensured with a swath equal to about 1,600 km. In any case, an orbital control strategy must be considered, as the higher harmonics of the lunar gravitational field give a significant variation of the satellite eccentricity (D'Avanzo et al., 1997) so the satellites of the constellation must have orbital control engines and enough propellant mass for orbit maintenance. Then it is of particular importance to reduce as much as possible the on-board propellant mass needed for the lunar transfer and for the final orbit injection. A convenient option is the use of the so-called weak stability boundary (WSB) lunar transfers. These transfers use low-energy orbits found by Belbruno (Belbruno, 1990) and already tested in a Japanese mission (Belbruno and Miller, 1990; Kawaguchi et al. 1995). Figure 1 shows an example of a WSB lunar transfer: in the origin is the Earth, and the circular orbit is the orbit followed by the Moon during the spacecraft transfer orbit.

Note that the spacecraft goes farther than 10^6 km from the Earth to take advantage of the Sun's gravitational effect; if the Sun's gravitational field is neglected, one would obtain the elliptical orbit shown in Fig. 1. In fact, the Sun increases the perigee of

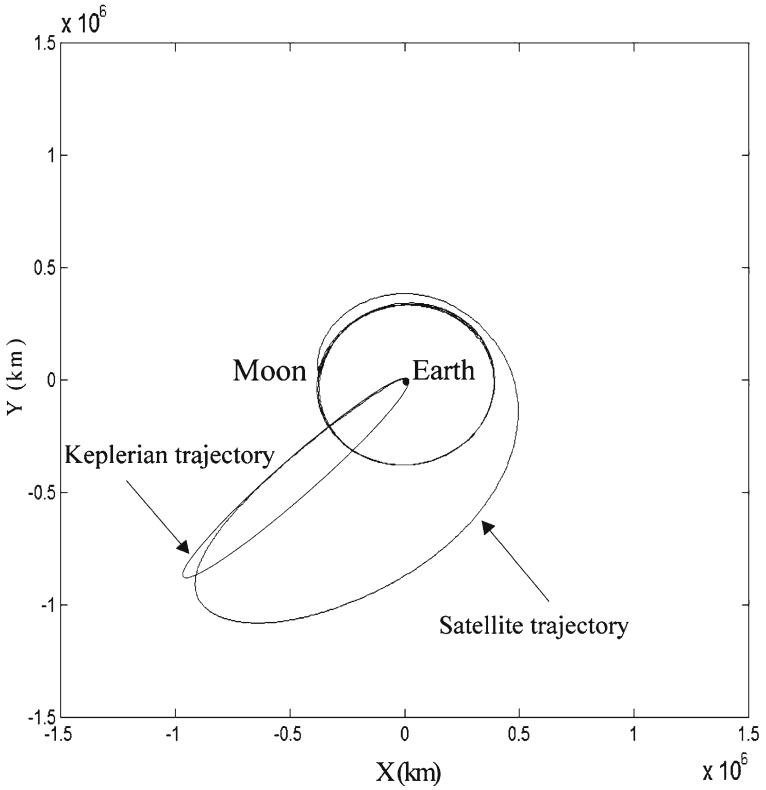

Fig. 1 A weak stability boundary (*WSB*) lunar transfer

the orbit until it reaches the moon's orbit radius, and it provides the spacecraft with just the right energy to allow a lunar ballistic capture. Therefore, the first ΔV given by the launcher at Earth departure, is bigger than the first impulse necessary for Hohmann-like transfer, but due to the ballistic capture, the braking ΔV at Moon, given by the satellite engine, is by far smaller, and thus about 20% of the on-board propellant mass can be saved (Belbruno, 2004). Some physical and analytical insights into the WSB dynamics can also be found in Kawaguchi et al. (1995), Koon et al. (2000, 2001), Circi and Teofilatto (2001), Koon et al. (2001).

Then, to save as much propellant as possible, a nominal WSB trajectory is used as a transfer trajectory to the moon and the satellites are spread on the planes of the constellation by small impulsive burns performed in different points of the nominal trajectory. It seems convenient to separate the satellites in a region of low gravitational field in the Earth–Moon–Sun system. It is expected that in such a region a small impulse produces rather different orbital parameters at Moon, so a substantial saving can be achieved with respect to a constellation deployment performed at Moon arrival. In fact the "weak stability" character of the nominal trajectory is such that small impulsive separation manoeuvres, corresponding to a variation of velocity of 20 cm/s (the separation velocity, which can be achieved by a small spring separation device), given at certain points of the nominal trajectory allow the formation of these 12 satellites in the two lunar constellation planes with a ΔV saving with respect to a classical constellation deployment strategy. Therefore, this strategy is proved to be effective for the kind of constellation considered (two planes). However, for a more general constellation design different strategies must be pursued. In fact, it is proved in the paper that the values of the final orbit parameter at the Moon are frozen to just two sets of values if impulses of the same intensity are performed at different points of the nominal trajectory, while keeping the periselenium altitude h_p fixed at a nominal value. This sort of regular behaviour seems to be surprising in the setting of "weakly stable" dynamics; however, it is shown that this behaviour is a common feature of the restricted two-, three- and four-body problems. In particular the restricted (bicircular) four-body problem can be considered a good approximation of the dynamics involved in a WSB dynamic trajectory.

This paper is organized as follows: in Sect. 2, the proposed strategy for the lunar constellation deployment is described and the ΔV saving with respect to a traditional manoeuvre is determined. In Sect. 3, it is shown that the orbital parameters at the Moon, obtained by small perturbation of a nominal WSB trajectory, are frozen to just two sets of values, if the periselenium distance is kept fixed. In Sects. 4 and 5, this property is proved to be common to other simpler dynamical systems, such as the Keplerian problem (Sect. 4) and the restricted three- and four-body problems (Sect. 5).

2 Lunar constellation deployment by WSB trajectories

The basic idea is to take advantage of the WSB dynamics to deploy a constellation of satellites at circular orbits of radius R saving as much propellant as possible. A feasible strategy is to consider a spacecraft on a WSB trajectory having the periselenium distance equal to R. For example, a constellation of satellites of commune radius $R = 1{,}938$ km is considered, then nominal WSB trajectory with periselenium altitude equal to 200 km polar orbit at Moon is chosen. The total ΔV needed to achieve a circular lunar orbit at 200 km of altitude, from a circular Earth orbit at 200 km of alti-

tude, using WSB transfers is 3.83 km/s ($\Delta V_1 = 3.19$ km/s, $\Delta V_2 = 0.64$ km/s). On the other hand, an ordinary Hohmann-like transfer having the same final parameters at Moon requires 3.98 km/s ($\Delta V_1 = 3.13$ km/s, $\Delta V_2 = 0.85$ km/s). It is important to note that the second impulse, at the moon pericentre, is given by the satellite, while the first one is given by the last stage of the launcher. For the second ΔV, the difference between WSB and classical transfer is about 200 m/s and this saving directly influences the satellite propellant mass. Then a substantial saving (about 20% of the on-board propellant mass) is achieved in reaching the polar lunar orbit of the satellite constellation. A numerical experiment is now executed to explore which lunar trajectories are attainable and what ΔV saving can be obtained in the constellation deployment performing small impulses along the nominal WSB transfer. For instance, let the effect of six impulses of 20 cm/s given along both the directions $(\pm\hat{c}_1, \pm\hat{c}_2, \pm\hat{c}_3)$ of each of the three inertial axes be considered. These impulses are simultaneously performed at a point in the nominal trajectory. In the present example, such a point corresponds to 44 days of transfer time. In Fig. 2, the point of the nominal trajectory where the six impulses have been simultaneously performed is shown (separation time). Even if the relative ΔV between the six trajectories is rather small, their relative distance increases with time and the six trajectories have different approaches to the Moon.

In fact, three of the six trajectories miss the lunar capture: these are the trajectories generated by the impulses given along the $\hat{c}_1, -\hat{c}_2, -\hat{c}_3$ directions. The other three trajectories, generated by impulses given along the $-\hat{c}_1, \hat{c}_2$, and $\hat{c}_3$, directions, are captured and the parameters are shown in Table 1 together with their nominal trajectory parameters. Note that different periselenium altitudes and angles, inclination and nodal angles are achieved at Moon.

In the hypothesis of a constellation of circular orbits of commune radius R, it is convenient to select only those impulses generating trajectories with periselenium height h_p close to the nominal trajectory periselenium altitude $h_p = 200$ km (so $R = 200 + 1{,}738$ km is equal to the circular orbit radius required by the constella-

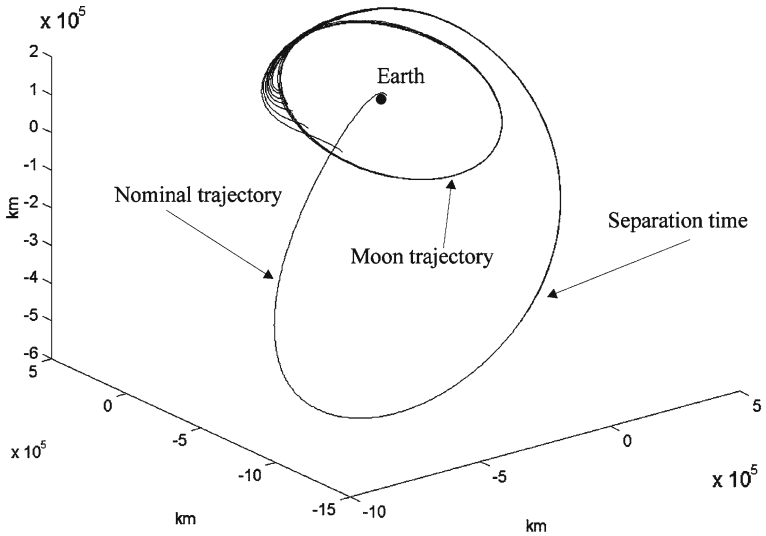

Fig. 2 The reference weak stability boundary (*WSB*) lunar transfer

Table 1 Orbital parameters at moon pericentre

Trajectory	h_p (km)	Transfer time (days)	a (km)	e	i (deg)	Ω (deg)	ω (deg)	ϑ (deg)
Nominal	203	91.92	32,909	0.941	89.99	0.033	120	−8.33
$-\hat{c}_1$	589	90.85	37,158	0.937	55.36	143.15	177.42	5.49
$\hat{c}_2$	14,327	90.45	47,813	0.663	52.79	167.08	50.62	12.13
$-\hat{c}_3$	2,293	90.72	38,542	0.895	55.02	152.28	72.25	−5.23

tion design). In fact, only orbits with $h_p < 1{,}000$ km will be considered: one can see that just one of these six trajectories satisfies such a requirement. This trajectory has $h_p = 589$ km, inclination $i = 55°$ and $\Omega = 143°$, and so a variation of inclination and Ω is achieved with a small variation of velocity ΔV. Note that a global lunar coverage can be achieved with seven satellites on the nominal lunar orbit (that has parameters $i_1 = 90°, \Omega_1 = 0°$), and five satellites on the varied orbit ($i_1 = 55°, \Omega_1 = 143°$) and all circular orbits at $R = 1{,}938$ km.

Note that to reduce the periselenium altitude from 598 km to the nominal altitude (200 km), one needs only 5 m/s. Using a traditional strategy the same coverage properties can be obtained by varying, for example, the inclination at aposelenium of the nominal trajectory. Then a variation of velocity 122 m/s is needed for every satellite to be set in the non-nominal plane. Therefore, according to this constellation design, five satellites increase the total required ΔV by about 600 m/s.

3 Separation manoeuvre on WSB lunar transfer

This constellation deployment has been realized with an impulse given in direction $-\hat{c}_1$ performed after 44 days of transfer time. To determine if alternative lunar satellite configurations can be achieved changing the separation time, the nominal trajectory is divided into 416 points, corresponding to the steps of the numerical integration. Moreover, to investigate the effect of the different possibilities, 18 impulsive burns, rather than six, are given at every point of the trajectory. The 18 burns are given in both the directions of each of the inertial reference system axes ($\pm\hat{c}_1, \pm\hat{c}_2, \pm\hat{c}_3$), and in the diagonal directions ($\pm\frac{\sqrt{2}}{2}\hat{c}_i \pm \frac{\sqrt{2}}{2}\hat{c}_j$), $i, j = 1, 3, i < j$, and they have been enumerated according to Table 2.

The burns have all the same intensity equal to $\Delta V = 20$ cm/s. In Fig. 3, sequences of burns performed at different points of the nominal trajectory are shown: the burns

Table 2 Burns direction

1	2	3	4	5	6
$\hat{c}_1$	$-\hat{c}_1$	$\hat{c}_2$	$-\hat{c}_2$	$\hat{c}_3$	$-\hat{c}_3$
7	8	9	10	11	12
$\frac{\sqrt{2}}{2}\hat{c}_1 + \frac{\sqrt{2}}{2}\hat{c}_2$	$\frac{\sqrt{2}}{2}\hat{c}_1 - \frac{\sqrt{2}}{2}\hat{c}_2$	$-\frac{\sqrt{2}}{2}\hat{c}_1 + \frac{\sqrt{2}}{2}\hat{c}_2$	$-\frac{\sqrt{2}}{2}\hat{c}_1 - \frac{\sqrt{2}}{2}\hat{c}_2$	$\frac{\sqrt{2}}{2}\hat{c}_2 + \frac{\sqrt{2}}{2}\hat{c}_3$	$\frac{\sqrt{2}}{2}\hat{c}_2 + \frac{\sqrt{2}}{2}\hat{c}_3$
13	14	15	16	17	18
$-\frac{\sqrt{2}}{2}\hat{c}_2 + \frac{\sqrt{2}}{2}\hat{c}_3$	$-\frac{\sqrt{2}}{2}\hat{c}_2 - \frac{\sqrt{2}}{2}\hat{c}_3$	$\frac{\sqrt{2}}{2}\hat{c}_1 + \frac{\sqrt{2}}{2}\hat{c}_3$	$-\frac{\sqrt{2}}{2}\hat{c}_1 + \frac{\sqrt{2}}{2}\hat{c}_3$	$\frac{\sqrt{2}}{2}\hat{c}_1 - \frac{\sqrt{2}}{2}\hat{c}_3$	$-\frac{\sqrt{2}}{2}\hat{c}_1 - \frac{\sqrt{2}}{2}\hat{c}_3$

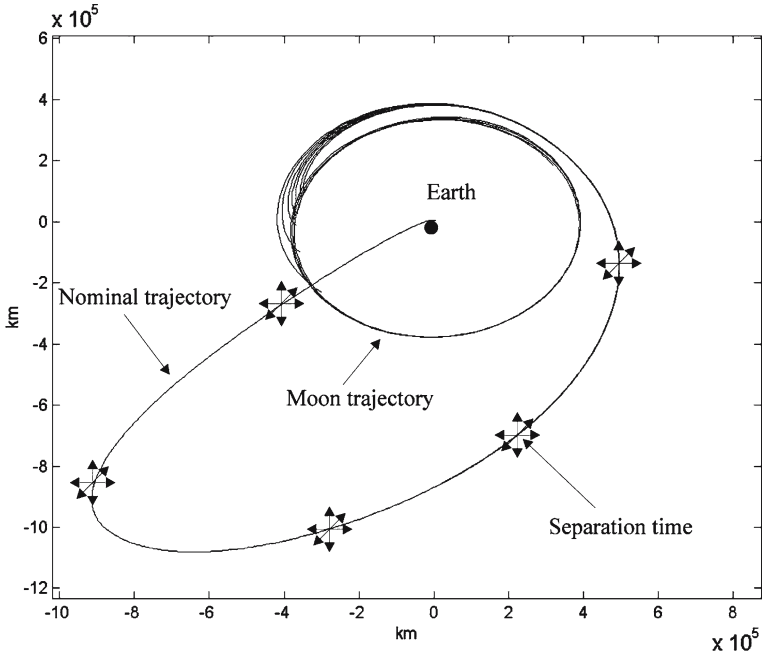

Fig. 3 Sequence of burns on the nominal trajectory at different times

are depicted by a cluster of arrows. Only those burns that produce a periselenium altitude h_p close to the nominal value are taken into account, and in Fig. 4 the final lunar parameters of the trajectories separated from the nominal WSB trajectory at different times are shown.

Note that a close-to-nominal altitude is achieved by only a few of the 18 trajectories generated at each separation time. Moreover, these trajectories have parameters at the Moon close to one of the two sets of parameters:

$$\begin{aligned} &i = 90°,\ \Omega = 0°,\ \omega = 120° \quad \text{(nominal WSB trajectory)} \\ &i = 55°,\ \Omega = 140°,\ \omega = 170° \quad \text{(varied WSB trajectory)} \end{aligned} \tag{1}$$

Figures 5–7 determine which of the 18 burns and at which separation time, lead to lunar capture with close-to-nominal altitude: in fact, the numbers over the circled points refer to the burn direction. For instance, in the range of separation time from 0 to 10 days, the successful burns are initially in direction 8, then in direction 17 and finally in direction 15. To give more physical insight into these results, Fig. 5 shows the angle between the burn direction and the velocity direction $\hat{v}$ of the nominal trajectory at burn time. Figure 6 shows the angle between the burn direction and the normal to the trajectory plane $\hat{h}$, and Fig. 7 shows the angle between the burn direction and the normal to the velocity direction in the trajectory plane $\hat{l}$.

For instance, let us consider in Fig. 5 the burn direction 2 occurring between the separation time 40 days and the separation time 60 days. The angle between the burn and the velocity direction varies approximately from 150° to 180°. Figure 6 shows that the burn direction 2 is in the trajectory plane (since the angle of the burn direction

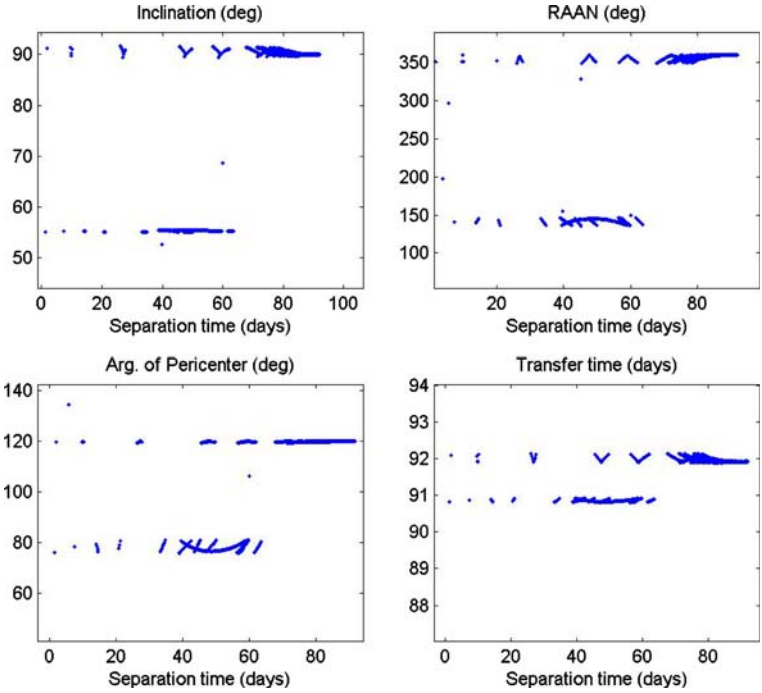

Fig. 4 Orbital parameters at Moon for different separation times from the nominal trajectory

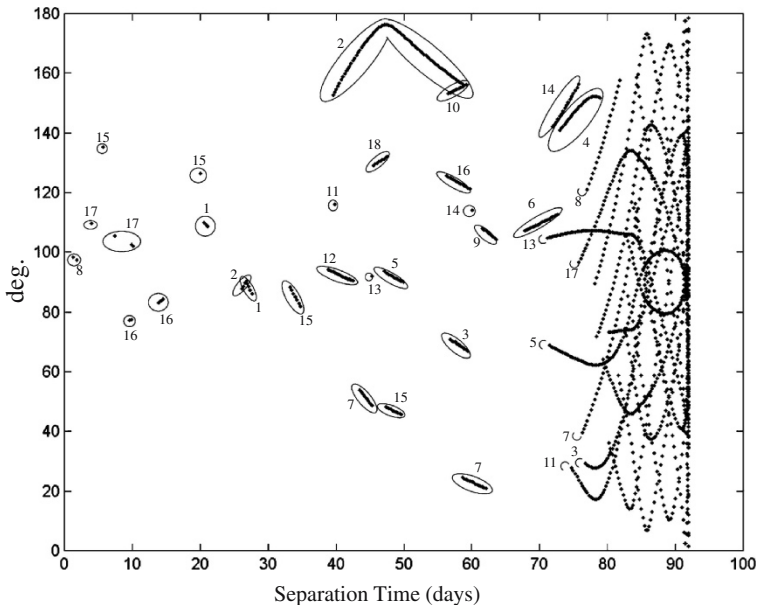

Fig. 5 Successful burn directions and their angle with respect to velocity direction

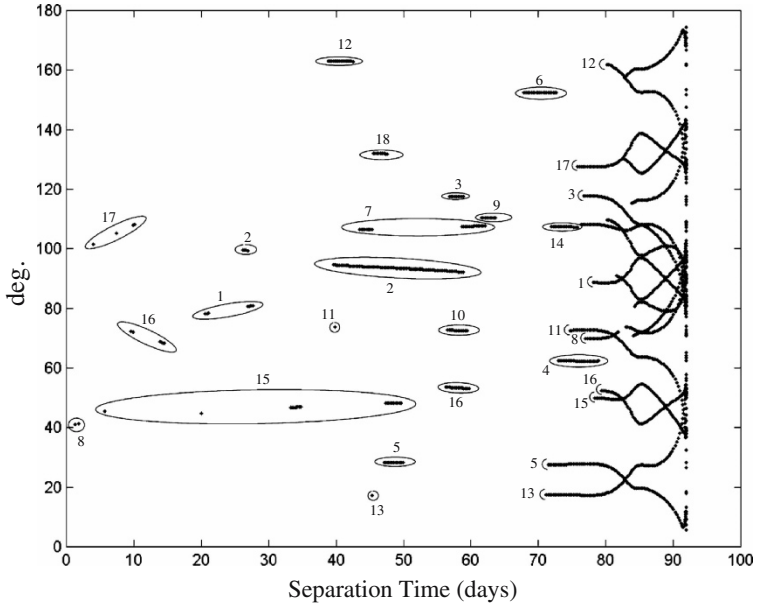

Fig. 6 Successful burn directions and their angle with respect to $\hat{h}$

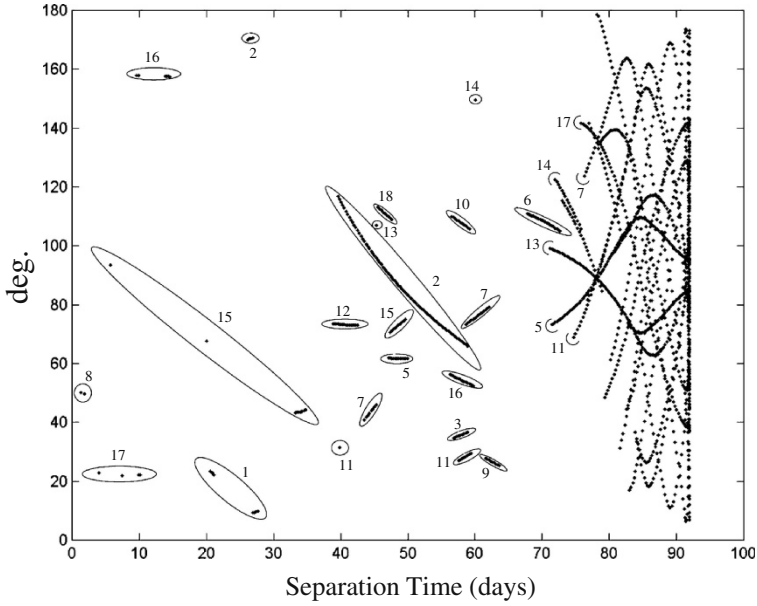

Fig. 7 Successful burn directions and their angle with respect to $\hat{l}$

angle with the normal to the trajectory plane is almost 90°) and then Fig. 7 shows the complementary of the angle of Fig. 5. This successful burn strategy is reported in Fig. 8 (braking impulsive burns). Note that in the same range of separation time (from 40 to 60 days) the successful burn direction 12 is parallel to $-\hat{h}$. Other possibilities can be determined by inspection of Figs. 5–7.

It turns out that several satellites can be set into the varied orbit (1) performing small impulsive separation burns. Moreover, such a manoeuvre can be performed at several different points of the nominal trajectory. To summarize, the proposed lunar constellation deployment seems to be rather convenient since:

- There is large freedom in the satellite separation time.
- The strategy is effective in terms of ΔV.

4 Families of trajectories in the Keplerian problem

The separation manoeuvre determined in the previous section is convenient for satellite constellation consisting of two planes. If the constellation design requires other orbital planes one could think of applying the same strategy, performing different impulses at different points of the nominal trajectory. However, Fig. 4 shows that

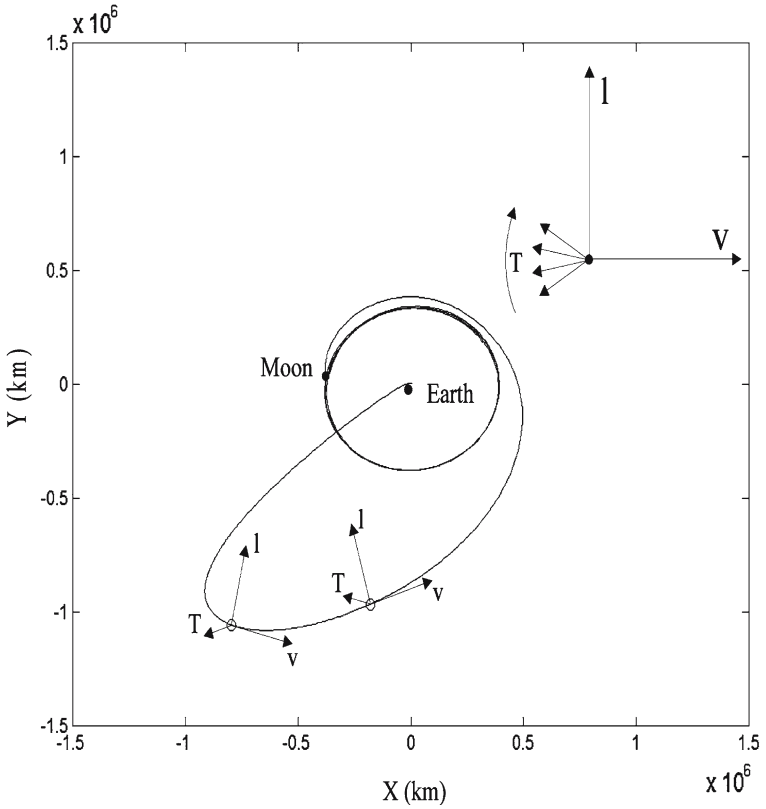

Fig. 8 Burn direction 2 at separation time from 40 to 60 days

it is not possible to vary the final orbit parameters i and Ω performing impulses of the same intensity at different points of the nominal trajectory, while maintaining h_p close to the nominal value. It seems a bit surprising to see such a result in the setting of "weakly stable" dynamics. In fact, these results show that there exists just two families of trajectories generated by small ΔV performed on a nominal WSB lunar transfer: (1) close-to-nominal trajectories (nominal family), (2) trajectories having Moon parameters similar to (1) (varied family). These two families have the following features:

(1) All the trajectories in both the families have almost the same periselenium altitude.
(2) The parameters i, Ω, ω of the nominal family are different with respect to the parameters of the varied family.

In this section, an attempt is made to understand such dynamical behaviour. Results will be obtained in simpler dynamical systems; in particular the Keplerian case will be analysed first. Families of trajectories passing through the same initial point $\mathbf{r}_0$ and having the same pericentre distance $\mathbf{r}_1$ will be determined. Of course, the orbits of these families will have different semimajor axes a and eccentricities e; the values of the perigee argument ω will be characterized. To define Keplerian orbits connecting point $\mathbf{r}_0$ to pericentre $\mathbf{r}_1$, let ϕ be the transfer angle between the two vectors (Fig. 9). Then the Keplerian conic from $\mathbf{r}_0$ to $\mathbf{r}_1$ has parameters (Battin, 1987):

$$e = \frac{1 - \frac{\mathbf{r}_0}{\mathbf{r}_1}}{1 - \frac{\mathbf{r}_0}{\mathbf{r}_1}\cos(\phi)}, \quad a = \frac{\mathbf{r}_1}{1 - e} \tag{2}$$

and the velocity V_0 at $\mathbf{r}_0$ of a direct orbit has radial and tangential velocity:

$$\begin{aligned} V_r &= -\sqrt{\frac{\mu}{\mathbf{r}_0}}\frac{e\sin(\phi)}{\sqrt{1+e\cos(\phi)}} \\ V_\vartheta &= -\sqrt{\frac{\mu}{\mathbf{r}_0}}\sqrt{1+e\cos(\phi)} \end{aligned} \tag{3}$$

Varying the transfer angle ϕ in (3) one gets the velocities at $\mathbf{r}_0$ to reach pericentre $\mathbf{r}_1$. The velocities (3) draw a hyperbola in the (V_r, V_ϑ) plane and the equal energy curves are just circles of radius $V_0 = \sqrt{{V_r}^2 + {V_\vartheta}^2}$. Figure 10 shows the hyperbola and some equal energy curves for $\mathbf{r}_0 = 10^6$ km and $\mathbf{r}_1 = 384,400$ km (approximately the Earth–Moon distance).

The branch of hyperbola with radial velocity $V_r > 0$ corresponds to orbits where $\mathbf{r}_0$ is after the pericentre; in the other branch ($V_r < 0$) the spacecraft at $\mathbf{r}_0$ is before the pericentre. The point $V_r = 0$ corresponds to $\mathbf{r}_0$ at apogee ($\phi = \pi$) and defines the minimum energy (Hohmann) transfer from $\mathbf{r}_0$ to $\mathbf{r}_1$. Note that elliptic transfer is possible only for $\mathbf{r}_0$ in the apogee region. The equal energy curves intersect the velocity locus hyperbola at two points: such intersection points are close only if the orbit in $\mathbf{r}_0$ is close to the minimum energy orbit transfer. In such a case with a small ΔV, it is possible to switch from one branch of the velocity locus to the other. Of course, the burn direction that produces such a ΔV must be given in an appropriate direction. Namely if (f_r, f_ϑ) are the radial and tangential components of the burn performed at the true anomaly ϑ of an orbit of parameters $(a, e, \omega, i, \Omega)$, then the variation of these parameters can be found according to the planetary Lagrange equations; in particular,

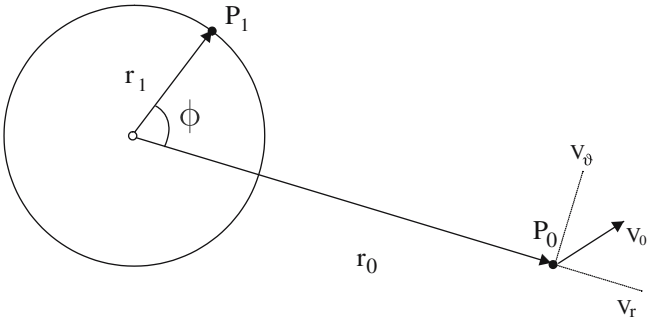

Fig. 9 Transfer angle from $\mathbf{r}_0$ to $\mathbf{r}_1$

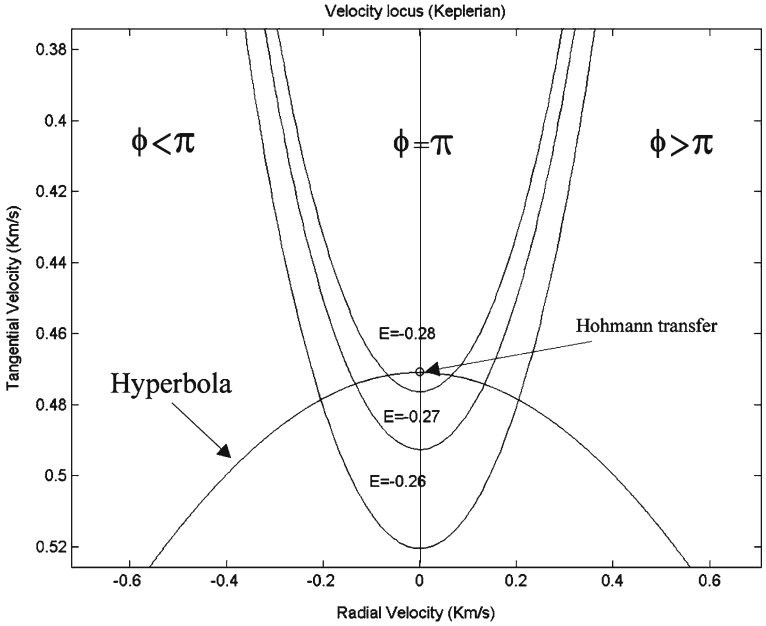

Fig. 10 Velocity locus for the Keplerian orbits

$$\begin{aligned}
\dot{a} &= \frac{2a^2}{h}\left[ef_r \sin(\vartheta) + (1 + e\cos(\vartheta))f_\vartheta\right] \\
\dot{e} &= \frac{r}{h}\left[\left(e + \cos(\vartheta) + \frac{h^2}{\mu r}\cos(\vartheta)\right)f_\vartheta + \frac{h^2}{\mu r}f_r \sin(\vartheta)\right] \\
\dot{\omega} &= \frac{r}{he}\left[\sin(\vartheta)(2 + e\cos(\vartheta))f_\vartheta - \cos(\vartheta)(1 + e\cos(\vartheta))f_r\right]
\end{aligned} \tag{4}$$

If the burn must be such that the pericentre distance $r_\mathrm{p} = a(1-e)$ is constant, one has the equation $\dot{r}_\mathrm{p} = 0$, which leads to

$$\frac{\dot{a}(1-e)}{a} = \dot{e} \tag{5}$$

This relation leads to the (f_r, f_ϑ) components of the burn:

$$\frac{f_r}{f_\vartheta} = \frac{\dfrac{e+\cos(\vartheta)}{1+e\cos(\vartheta)} + \cos(\vartheta) - \dfrac{2(1+e\cos(\vartheta))}{1+e}}{\sin(\vartheta)\left(\dfrac{2e}{1+e} - 1\right)} \tag{6}$$

That is, to maintain a given pericentre distance, a burn given at point $\mathbf{r}_0$ of true anomaly ϑ and in a nominal orbit of semi-major a and eccentricity e, must have the direction defined by the angle σ taken from the radial direction $\hat{r}_0$, where $\sigma = a\tan(\frac{f_r}{f_\vartheta})$ and the ratio f_r/f_ϑ is given by (6). Then, one has the two relations:

$$\Delta V^2 = \Delta f_r^2 + \Delta f_\vartheta^2 \tag{7}$$

$$\Delta f_r = \pm\sqrt{\frac{\Delta V^2}{1+\dfrac{1}{\left(\dfrac{\Delta f_r}{\Delta f_\vartheta}\right)^2}}} \tag{8}$$

where $\dfrac{\Delta f_r}{\Delta f_\vartheta} = \dfrac{f_r}{f_\vartheta} = \Delta f_{r\vartheta}$ is equal to (6). Then, according to (4), the variation $\Delta\omega$ of perigee argument of the nominal orbit is equal to:

$$\Delta\omega = \pm\frac{h}{\mu e}\frac{\sqrt{\frac{\Delta V^2}{1+\frac{1}{(\Delta f_{r\vartheta})^2}}}}{(1+e\cos(\vartheta))} \left[\frac{\sin(\vartheta)^2(2+e\cos(\vartheta))\left(\dfrac{2e}{1+e}-1\right)}{\dfrac{e\cos(\vartheta)}{1+e\cos(\vartheta)}+\cos(\vartheta)-\dfrac{2(1+e\cos(\vartheta))}{1+e}} - \cos(\vartheta)(1+e\cos(\vartheta))\right], \tag{9}$$

where ϑ is the true anomaly of the point $\mathbf{r}_0(\vartheta)$ of the nominal orbit where the burn is performed. The plot of the variation of pericentre argument $\Delta\omega$ as point $\mathbf{r}_0$ varies on the nominal orbit (i.e., as the true anomaly ϑ, or the corresponding time, varies) is in Fig. 11 where the variation of velocity produced by the impulsive burn is $\Delta V = 20$ cm/s. Note that in the Keplerian model $\Delta\omega$ is proportional to ΔV and that only two solutions exist.

In this figure, a continuous variation of argument of pericentre is shown, different from the behaviour of ω in Fig. 4. However, it turns out that close to pericentre there is an almost zero variation $\Delta\omega$; that is, the argument of pericentre stays close to the nominal value, as can be seen for the WSB case of Fig. 4 (the nominal family). Moreover, at the apocentre region (corresponding to about 40 days), the rate of variation of ω decreases; that is, the burns about the apogee region produce almost the same pericentre arguments, as happens in Fig. 4 (the varied family).

5 Families of trajectories in the restricted three- and four-body problem

In the restricted three-body problem setting, the definition of orbits connecting point $\mathbf{r}_0$ to a fixed pericentre distance has already been discussed in Hadjidemetriou (1968), where $\mathbf{r}_0$ is in the inner Lagrangian point L_1 and a complete classification of

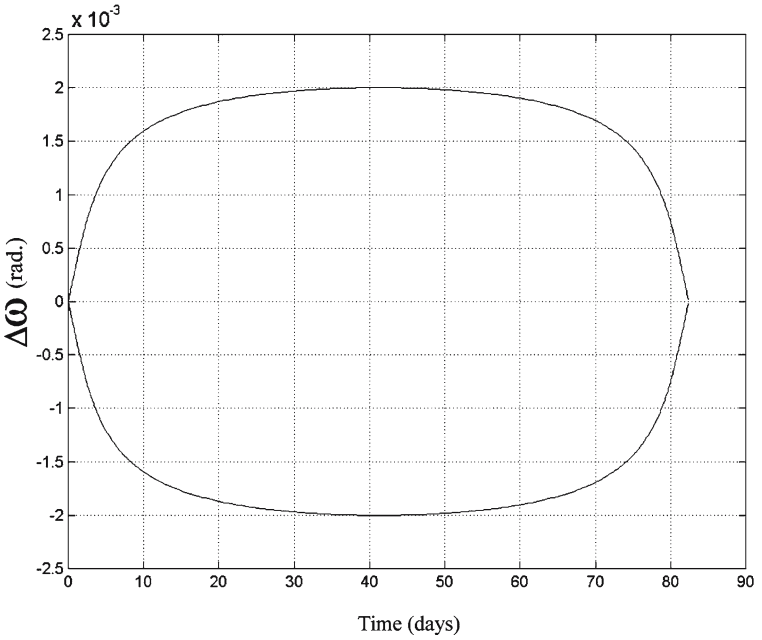

Fig. 11 Argument of pericentre variation for different values of burn point $\mathbf{r}_0$

two- and three-dimensional orbits according to their pericentre distance from both primaries is given. Note that in the same reference an analytic formula for the velocities V_0 needed to reach a pericentre distance $\mathbf{r}_1$ from a satellite in position $\mathbf{r}_0$ was given for the two-body problem defined in a reference frame rotating with unitary angular velocity ω_1:

$$\mathbf{r}_1^2\left[V_0^2 + 2V_0 \cdot \omega_1 \times \mathbf{r}_0 + (\omega_1 \times \mathbf{r}_0)^2 - 2\right] + 2\mathbf{r}_1 - \frac{1}{4}\left[\mathbf{r}_0^2 + \frac{2}{r_0} - 2 + 2V_0 \cdot \omega_1 \times \mathbf{r}_0 + (\omega_1 \times \mathbf{r}_0)^2\right]^2 = 0 \tag{10}$$

(for $\mathbf{r}_0$ in L_1, one recognizes (23) of Hadjidemetriou (1968)). A numerical search is developed here in the restricted three-body problem related to the Earth–Moon system with $\mathbf{r}_0 = 10^6$ km (made dimensionless with respect to the average Earth–Moon distance EM = 384,400 km) having an angle of $-40°$ with respect to the Earth–Moon axis. The final point $\mathbf{r}_1$ is any point with periselenium of distance $R = 1{,}938$ km from the Moon centre of mass (dimensionless with respect to Earth–Moon). The reference frame used is the usual frame rotating with the Earth–Moon system (Fig. 12), with coordinate position (x, y) dimensionless with respect to the average Earth–Moon distance EM = 384,400 km, and dimensionless time $\tau = t/\omega_{\mathrm{EM}}$ (where ω_{EM} is the angular velocity of the Earth–Moon system), so the component velocities (u, v) are dimensionless with respect to the average lunar velocity.

Figure 13 gives the horizontal and vertical velocities (u_0, v_0) at $\mathbf{r}_0$ in order to reach periselenium distance $\mathbf{r}_1$. The hyperbola of the Keplerian case (Fig. 10) shrinks into a curve with two branches that are close to each other. Note that with a small ΔV, it is possible to shift from one branch to the other.

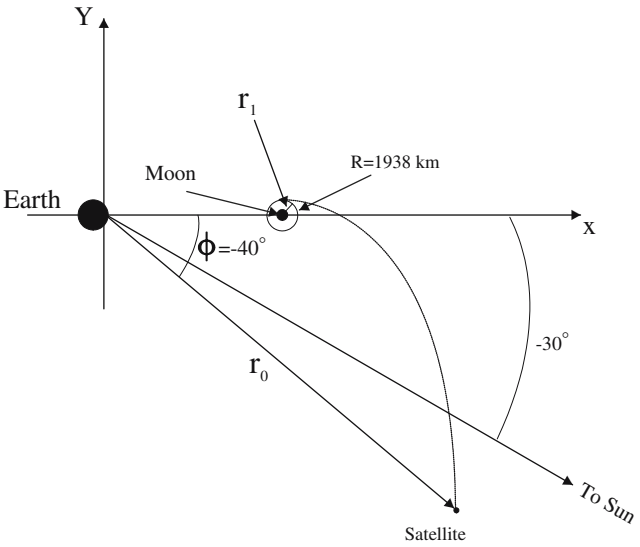

Fig. 12 Rotating Earth–Moon reference frame

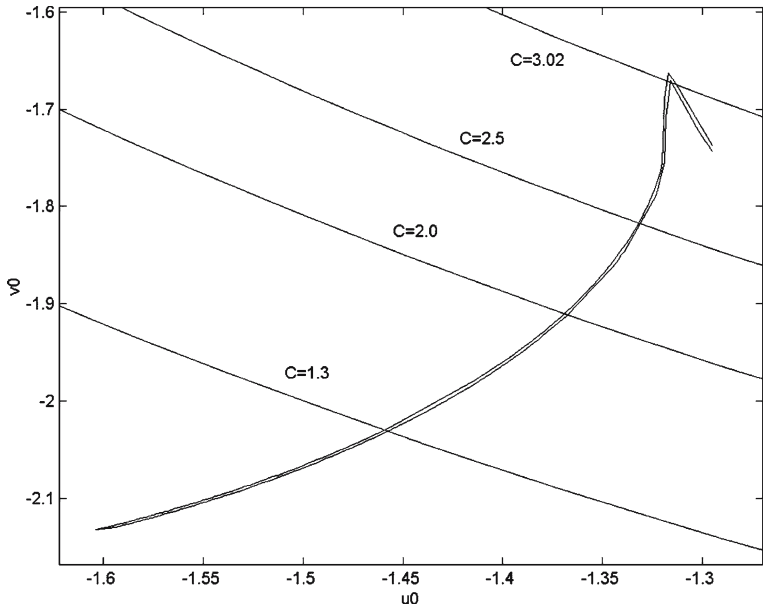

Fig. 13 Velocity locus (three-body problem, dimensionless velocities u_0, v_0)

In the velocity locus of Fig. 13, the equal Jacobi constant curves are shown. These curves are circles centred on the origin: note that the minimum energy transfer from $\mathbf{r}_0$ to the Moon, has Jacobi constant close to the value of the external Earth–Moon L_2 lagrangian point, so the upper region of the locus represents lunar transfer orbits with rather low energy. The transfer orbits of each of the two branches of the velocity locus have almost equal periselenium arguments ω; however, the value ω of the

upper branch is different from the ω value of the lower branch, the variation being $\Delta\omega \simeq 100°$ (Fig. 14).

It follows that with a small variation of velocity ΔV it is possible to have a lunar transfer with the same periselenium distance, but rather different periselenium arguments. Different from the Keplerian case, such a possibility holds true for rather different energy values (Jacobi constant values) of the transfer orbit. The same analysis has been made taking into account the Sun's gravitational field in the so-called bicircular restricted four-body problem (Simò et al. 1995; Kazuyuki 2004). That is, the Earth–Moon system is rotating in circular orbit about the Sun and the Moon is rotating around the Earth in a circular orbit in the same plane. The reference system has its origin in the Earth–Moon system. It is rotating with angular velocity ω_{EM}, and position and time are dimensionless as in the Earth–Moon-restricted three-body problem. The same initial and final positions of the three-body problem are considered; that is, $\mathbf{r}_0 = 10^6$ km (made dimensionless with respect to the average Earth–Moon distance, EM), with angle of $-40°$ with respect to the Earth–Moon axis, the final point $\mathbf{r}_1$ is a periselenium of distance $R = 1{,}938$ km from the Moon (dimensionless with respect to EM) and the Sun is initially at angle $-30°$ from the Earth–Moon axis (Fig. 12). Because of such a configuration, the Sun's gravitational field will brake the spacecraft during the final lunar approach to allow ballistic capture (Circi and Teofilatto, 2001).

A two-dimensional search on the velocity components (u_0, v_0) is carried out in order to reach the Moon from $\mathbf{r}_0$ with periselenium distance $R = 1{,}938$ km using the following equations of the bicircular problem (with $z_0 = w_0 = 0$):

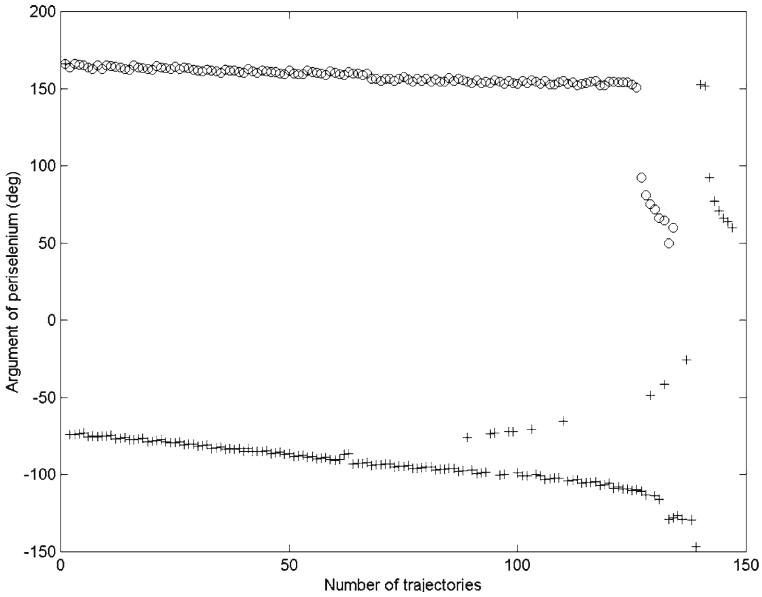

Fig. 14 Periselenium argument of the orbits in the velocity locus mentioned in text

$$
\begin{aligned}
\dot{x} &= u \\
\dot{y} &= v \\
\dot{z} &= w \\
\dot{u} &= 2v + x - \frac{1-\mu}{r_{\mathrm{E}}^3}(x+\mu) - \frac{\mu}{r_{\mathrm{M}}^3}(x-1+\mu) - \frac{m_S}{r_{\mathrm{S}}^3}(x-\rho\cos(\theta)) - \frac{m_S}{\rho^2}\cos(\theta) \\
\dot{v} &= -2u + y - \frac{1-\mu}{r_{\mathrm{E}}^3}y - \frac{\mu}{r_{\mathrm{M}}^3}y - \frac{m_S}{r_{\mathrm{S}}^3}(y-\rho\sin(\theta)) - \frac{m_S}{\rho^2}\sin(\theta) \\
\dot{w} &= -\frac{1-\mu}{r_{\mathrm{E}}^3}z - \frac{\mu}{r_{\mathrm{M}}^3}z - \frac{m_S}{r_{\mathrm{S}}^3}z \\
\dot{\theta} &= \omega_{\mathrm{S}}\tau
\end{aligned}
\tag{11}
$$

where (Fig. 15)

$$
\begin{aligned}
r_{\mathrm{E}} &= \sqrt{(x+\mu)^2 + y^2 + z^2} \\
r_{\mathrm{M}} &= \sqrt{(x-1+\mu)^2 + y^2 + z^2} \\
r_{\mathrm{s}} &= \sqrt{(x-\rho\cos(\theta))^2 + (y-\rho\sin(\theta))^2 + z^2} \\
\rho &= 389.2, \mu = 0.01215, m_{\mathrm{S}} = 3.298 \cdot 10^5
\end{aligned}
\tag{12}
$$

Figure 16 shows the four-body problem velocity locus; this looks rather similar to the three-body velocity locus of Fig. 13.

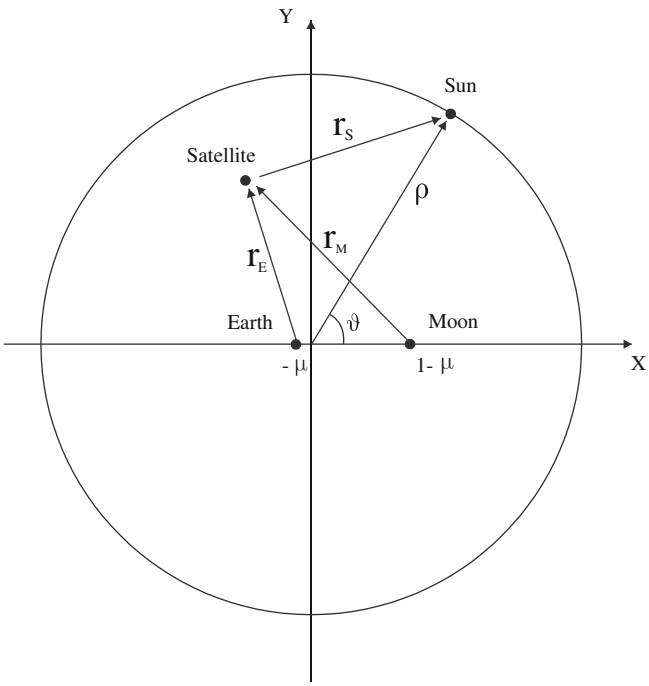

Fig. 15 Reference system in a bicircular model

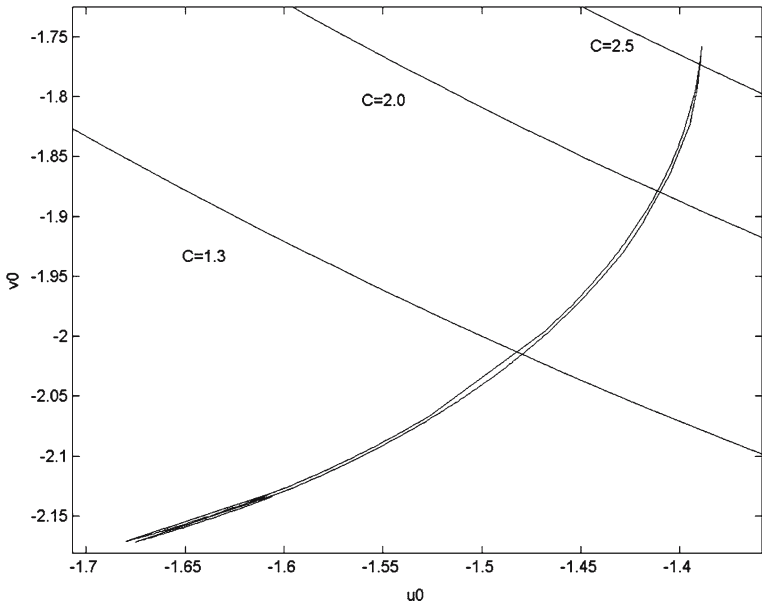

Fig. 16 Velocity locus (restricted four-body problem, dimensionless velocities u_0, v_0)

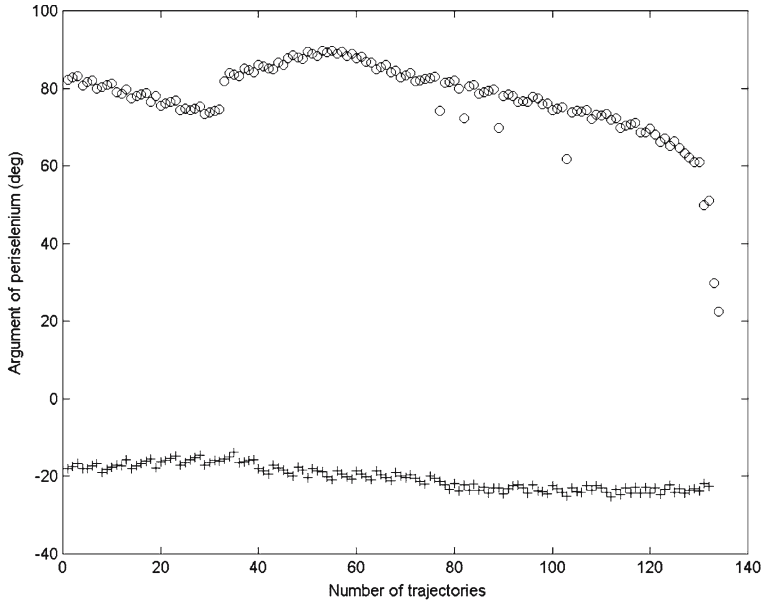

Fig. 17 Periselenium argument of the orbits in the velocity locus mentioned in text

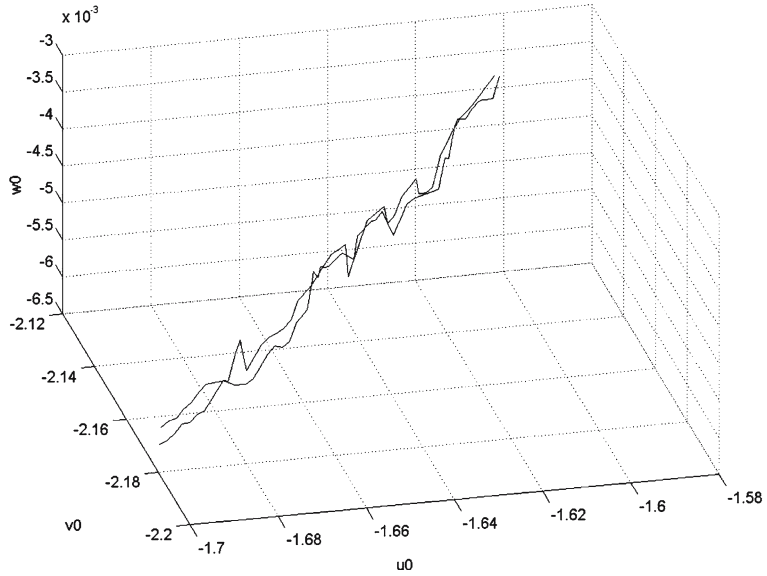

Fig. 18 Three-dimensional velocity locus (restricted four-body problem, dimensionless velocities)

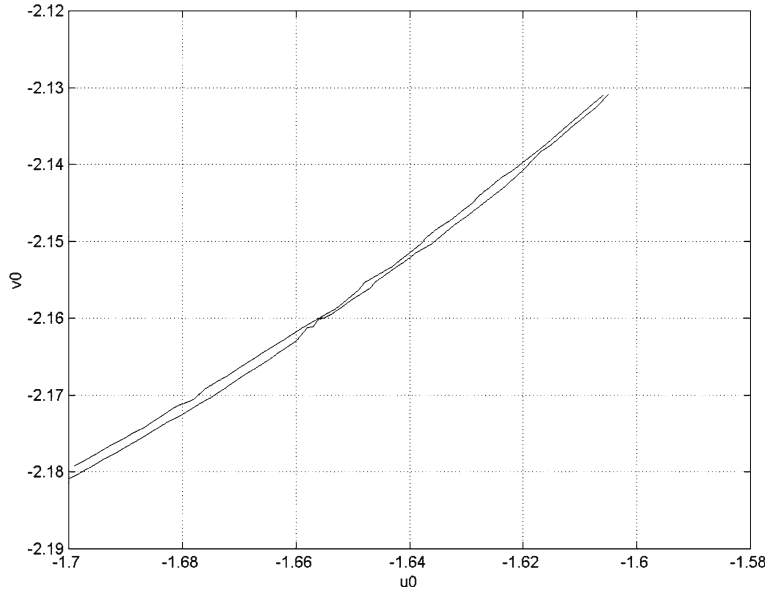

Fig. 19 Velocity locus: planar (u_0, v_0) projection of Fig. 18

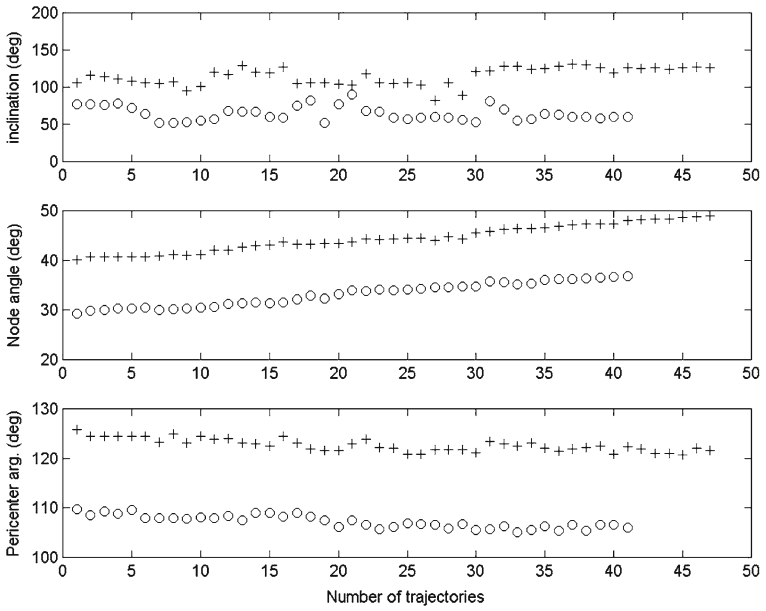

Fig. 20 Orbital parameters of the two families of Fig. 18

In Fig. 16, two families of trajectories can be again identified: in fact, as in the three-body problem case, two branches in the velocity locus are apparent. In Fig. 17, the periselenium argument of trajectories belonging to the two families is shown. Note that there is a difference of about 100° between the ω of the two families, as occurs in the three-body problem (Fig. 14).

Finally, a search on the three-dimensional components $u_0, v_0, w_0 \neq 0$ of the velocity $\mathbf{V}_0$ at $\mathbf{r}_0$ needed to reach the periselenium altitude r_1 is performed. The three-dimensional velocity locus is in Fig. 18. The planar u_0, v_0 projection of Fig. 18 is in Fig. 19, and it turns out to be qualitatively similar to the planar result of Fig. 16.

In this three-dimensional case, different parameters can be compared, such as inclination i, node angle Ω and the argument of perigee ω. Figure 20 shows that the orbital parameters in each of the two branches are similar, whereas the two branches have different orbital parameters.

6 Conclusions

A strategy for a lunar satellite constellation deployment is proposed, using a WSB lunar transfer and small perturbations from such a trajectory. The strategy is proved to be feasible and economical if the constellation design requires just two different orbital planes and for every satellite in a varied orbit about 120 m/s of ΔV are saved. The orbital parameters at the Moon obtained by small perturbation of a nominal WSB trajectory are frozen to a unique set of values, if the periselenium distance is kept fixed. Such a property resembles what happens in simpler dynamical systems. In fact, in the Keplerian problem families of trajectories having the same pericentre distance define a hyperbola in the velocity locus. The variation in perigee argument is as small

as is the intensity of the burn and it varies in a continuous way with the point where the burn is performed. However, it is possible to note that if the burn is performed around the pericentre region, the pericentre argument ω of the varied trajectory is almost equal to the pericentre argument of the nominal trajectory. If the burn is about the apocentre region, the angle ω of the varied trajectory is different from the nominal one and all the varied trajectories separated from the nominal trajectory at the apocenter region have almost the same ω. These features are amplified in the restricted three- and four-body problem. It is shown that trajectories having the same pericentre distance define two families in the velocity locus. The variation in perigee argument is large if one shifts from one family to the other, and this can be done with a small variation of velocity. Considering a three-dimensional case, it is possible to compare other orbital parameters, such as inclination and node angles. Again, each family is defined by common values of orbital parameters that vary from one family to the other.

References

Battin, R.H.: An introduction to the mathematics and methods of astrodynamics. AIAA Education Series, New York (1987)

Belbruno, E.: Examples of nonlinear dynamics of ballistic capture in the Earth-Moon system. AIAA Paper no. 2896 (1990)

Belbruno, E., Miller, J.: A ballistic lunar capture trajectory for the Japanese spacecraft Hiten. JPL Report IOM 312/90.4–1317 (1990)

Belbruno, E.: Capture dynamics and chaotic motions in celestial mechanics, pp. 144–148. Princeton University Press, Princeton (2004)

Bussey, B., Spudis, P.: The lunar poles: mapping the future lunar base. Moon Base: a Challenge for Humanity, International Conference, Venice Workshop, 26–27 May (2005)

Circi, C., Teofilatto, P.: On the dynamics of weak stability boundary lunar transfers. Celest. Mech. Dyn. Astr. **79**(1), 41–72 (2001)

D'Avanzo, P., Teofilatto, P., Ulivieri, C.: Long term effects on lunar orbiter. Acta Astronautica **40**(1), 13–20 (1997)

Graziani, F.: LUNISAT: an university satellite to the Moon. Paper presented in CELMEC IV, San Martino al Cimino, Italy, 12 September (2005)

Hadjidemetriou, J.: A classification of orbits through L_1 in the restricted three body problem. The Astronomical J. **73**(2), 104–110 (1968)

Kawaguchi, J., Yamakawa, H., Uesugi, T., Matsuo, H.: On making use of lunar and solar gravity assist for lunar A and planet B missions. Acta Astronautica, **35**, 633–642 (1995)

Kazuyuki, Y.: Sun-perturbed earth-to-moon transfers with low energy and moderate flight time. Celest. Mech. Dyn. Astr. **90**(3–4), 197–212 (2004)

Koon, W., Lo, M., Marsden, J., Ross, S.: Dynamical system, the three- body problem and space mission design. International Conference on Differential Equations, Berlin (2000)

Koon, W., Lo, M., Marsden, J., Ross, S.: Low energy transfer to the moon. Celest. Mech. Dyn. Astr. **81**(1), 63–73 (2001)

Simò, C., Gomez, G., Jorba, A., Masdemont, J.: The bicircular model near the triangular libration point of the RTBP. In: Roy, A., Steves, B.A. (eds.) From Newton to Chaos, pp. 343–370. Plenum Press, New York (1995)